NANO LETTERS

Letter

pubs.acs.org/NanoLett

Amphiphilic Surface Modification of Hollow Carbon Nanofibers for Improved Cycle Life of Lithium Sulfur Batteries

Guangyuan Zheng,[†] Qianfan Zhang,[‡] Judy J. Cha,[‡] Yuan Yang,[‡] Weiyang Li,[‡] Zhi Wei Seh,[‡] and Yi Cui*[,‡,§]

[†]Department of Chemical Engineering and [‡]Department of Materials Science and Engineering, Stanford University, Stanford, California 94305, United States

[§]Stanford Institute for Materials and Energy Sciences, SLAC National Accelerator Laboratory, 2575 Sand Hill Road, Menlo Park, California 94025, United States

Supporting Information

ABSTRACT: Tremendous effort has been put into developing viable lithium sulfur batteries, due to their high specific energy and relatively low cost. Despite recent progress in addressing the various problems of sulfur cathodes, lithium sulfur batteries still exhibit significant capacity decay over cycling. Herein, we identify a new capacity fading mechanism of the sulfur cathodes, relating to Li_xS detachment from the carbon surface during the discharge process. This observation is confirmed by ex-situ transmission electron microscopy study and first-principles calculations. We demonstrate that this capacity fading mechanism can be overcome by introducing amphiphilic polymers to modify the carbon surface, rendering strong interactions between the nonpolar carbon and the polar Li_xS clusters. The modified sulfur cathode show excellent cycling performance with specific capacity close to 1180 mAh/g at C/5 current rate. Capacity retention of 80% is achieved over 300 cycles at C/2.

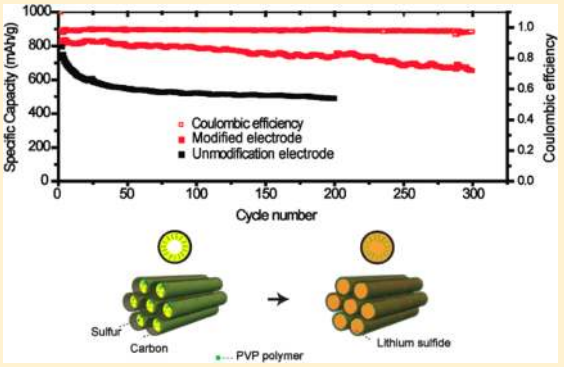

KEYWORDS: *Lithium sulfur batteries; energy storage; surface modification*

Increasing the energy density of lithium batteries has become an important focus of materials research, due to the urgent needs of energy storage for vehicle electrification and grid scale applications. To this end, lithium sulfur batteries can bring about significant improvements to the current state-of-the-art battery technologies in terms of higher specific capacity and cost saving.[1−4] Sulfur cathode has a specific capacity of around 1673 mAh/g, which gives lithium sulfur batteries a specific energy of around 2600 Wh/kg, much higher than the conventional lithium ion batteries based on metal oxide cathodes and graphite anodes. Commercial applications of lithium sulfur batteries have not been very successful despite several decades of research.[5] The major problems of sulfur cathode include low active material utilization, poor cycling performance and low Coulombic efficiency.[6] Much effort has thus been put into improving the electrochemical performance of the sulfur cathode. Of notable successes are the recent works by Nazar et al., who pioneered the developments of mesoporous carbon particles for sulfur encapsulation, and achieved a very high specific capacity of around 1300 mAh/g.[7,8] Other nanostructured carbon materials that have been shown to improve sulfur cathode performance include porous carbon spheres,[9,10] hollow carbon nanofibers,[11,12] activated carbon fiber,[13] and graphene oxides.[14,15] Several groups have also demonstrated that oxides additives, such as mesoporous silica,[16] titania,[17] and metal−organic framework (MOF)[18] can improve the sulfur cathode performance. In particular, modification of the sulfur electrode by polar polymer additives is consistently shown to improve the cycling performance.[7,15,19] Some hypotheses were proposed to explain the effect of the polymer additives, but there has been no specific evidence provided. The difficulty in elucidating the contributions of the polymer additives stem from the fact that it is very challenging to study the sulfur electrode at nanoscale, either by spectroscopic or microscopic methods. Sulfur can easily sublime under vacuum and lithium polysulfides are sensitive to both air and moisture. Recently, our group demonstrated a hollow carbon nanofiber/sulfur composite cathode structure that exhibited a high specific capacity of around 1500 mAh/g and improved cycle life. The hollow carbon nanofiber structure provides an ideal platform for studying the sulfur electrode at nanoscale. By confining the sulfur in the hollow carbon nanofibers, it is possible to carry out transmission electron microscopy (TEM) characterizations of the sulfur cathode without significant damage to the sample.

In this work, we investigated the structural change of the sulfur cathode using the hollow carbon nanofibers. It was observed that lithiation of sulfur resulted in the detachment of

Received: December 30, 2012
Revised: January 27, 2013

ACS Publications © XXXX American Chemical Society

dx.doi.org/10.1021/nl304795g | *Nano Lett.* XXXX, XXX, XXX−XXX

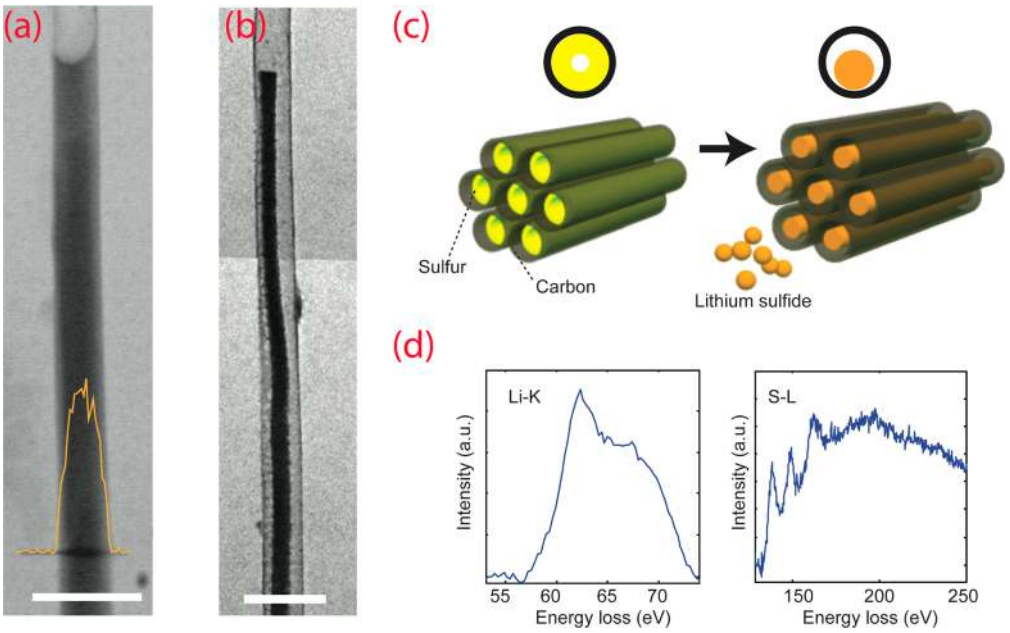

Figure 1. Ex situ study of hollow carbon nanofiber encapsulated sulfur cathode. (a) TEM image of the sulfur cathode before discharge. The yellow line represents the EDS counts of the sulfur signal along the dark line. (b) TEM image of the sulfur cathode after fully discharge to 1.7 V. The scale bars in parts a and b are 500 nm. (c) Discharge profile of the sulfur cathode. Insets are schematics showing the morphological change of sulfur cathode after discharge. (d) EELS signal of lithium K-edge and sulfur L-edge of the discharge sulfur cathode.

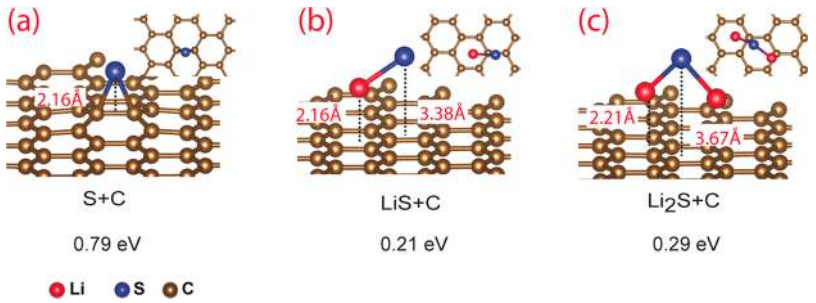

Figure 2. Theoretical calculation of molecular binding. First-principles calculations showing the interaction between the carbon surface and S (a), LiS (b), and Li_2S (c). The numbers represent the bond lengths between the sulfur atoms and the carbon surface in each case. The insets show the top views of the molecular configurations.

the lithium sulfide from the carbon surface, indicating the importance of interfacial effect in contributing to the sulfur cathode decay. We performed first-principles calculations to study how lithiation changes the chemical interaction between sulfur and the carbon surface. The results showed a significant decrease in binding energy between the lithium sulfide and the carbon. In light of this new understanding, we modified the interface between the carbon and sulfur with amphiphilic polymers and showed a much-improved cycling performance of the modified electrode.

Results and Discussion. *TEM Study.* Fabrication of the electrodes was based on our previously reported method (see Methods in the Supporting Information).[11] Figure 1a shows the TEM image of the sulfur-filled hollow carbon nanofiber. The yellow line indicates the energy-dispersive X-ray spectroscopy (EDS) counts of sulfur signal, which is distributed within the carbon fiber. The as-fabricated sulfur cathode was then assembled into a 2032-type coin cell (MTI) with lithium metal as the counter electrode. The electrolyte was 1 M lithium bis(trifluoromethanesulfonyl)imide (LiTFSI) and 1 wt % lithium nitrate ($LiNO_3$) in 1,3-dioxolane and 1,2-dimethoxyethane (volume ratio 1:1). The battery was discharged at C/5 current rate to 1.7 V and held at this voltage for another 24 h until the discharge current was smaller than 5 μA. The discharge profile (Figure S2, Supporting Information) exhibits the typical two-plateau behavior of sulfur cathode. The second plateau is relatively flat, indicating good reaction kinetics between the lithium and sulfur. Figure 1b shows the TEM image of a sulfur cathode after the first discharge. The inner core is identified as lithium sulfide based on the electron energy loss spectra (EELS), which show lithium K-edge and sulfur L-edge from the core (Figure 1d). The image shows clear shrinking of lithium sulfide away from the carbon wall along the length of the hollow nanofiber (Figure S3, Supporting Information). This observation is surprising as the density of lithium sulfide is lower than that of sulfur, which means that lithiated sulfur undergoes volumetric expansion.[20] Separation of lithium sulfide from the carbon wall means that the intermediate polysulfides could have leaked out from the hollow carbon nanofibers through the openings. The extra Li2S could have precipitated and segregated from the carbon matrix, resulting in the loss of electrical contact and capacity decay (Figure 1c).

dx.doi.org/10.1021/nl304795g | *Nano Lett.* XXXX, XXX, XXX–XXX

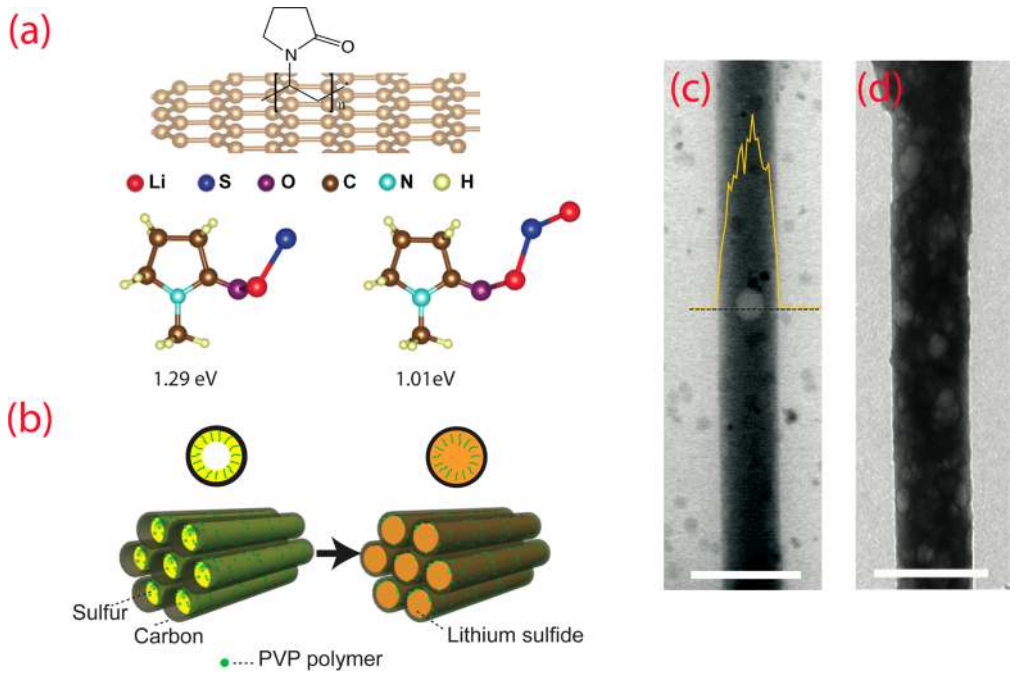

Figure 3. Results of the modified hollow carbon nanofiber with PVP. (a) Schematic showing the interaction between PVP and carbon surface (upper). First-principles calculation shows the interaction between the discharge products and the functional group on the polymer. (b) Schematics of the polymer modified sulfur cathode before (left) and after discharge (right). (c) TEM image of the sulfur cathode after functionalization with polymer and infusion of sulfur. The yellow line represents the EDS counts of sulfur signal along the dashed line. (d) TEM image of the sulfur cathode after fully discharge. The scale bars are 500 nm.

DFT Simulation. To elucidate the mechanism of lithium sulfide detachment, we performed first-principles calculation to study the interaction between the lithium sulfide species and the carbon surface. For simplicity, we used single-layer graphene as the modeling substrate to represent the carbon surface, and Li_xS ($0 \leq x \leq 2$) clusters as the models for the lithium sulfides species at discharge. The approach may not give an absolute quantification of the binding strength between the lithium sulfide species and the carbon surface, but will provide a qualitative understanding on the importance of interfacial effect on cycling performance. Figure 2 shows the most stable adsorption configuration for Li_xS when x = 0, 1, and 2. For single sulfur atom adsorption case (x = 0), the most stable position is the bridge site, on top of the C−C bond (Figure 2a). The calculated binding energy is 0.79 eV, in agreement with the previously reported result.[14] When sulfur reacts with lithium, there is a dramatic decrease in binding energy with the carbon surface. For LiS and Li_2S clusters, the distances between the sulfur atoms and the graphene surface are 3.38 Å and 3.67 Å, respectively (Figure 2, parts b and c), much larger than the 2.16 Å for elemental sulfur. The corresponding binding energies between Li_xS and the carbon surface are 0.21 eV (LiS) and 0.29 eV (Li_2S), smaller than that for elemental sulfur. The weakening of sulfur adhesion to the carbon surface, coupled with the increased ionic binding within the lithium sulfide compounds, leads to the detachment of lithium sulfides species from the carbon surface and self-aggregation during further discharge process. Precipitation of lithium sulfide thin film on top of the sulfur electrode has been reported in several previous studies,[21−23] which are in line with the prediction of material segregation between carbon and lithium sulfide.

The results suggest that the interfacial effect between the lithium sulfide and the carbon can play important role in sulfur cathode degradation. Dissolution of lithium polysulfides has long been understood to be the major problem of sulfur cathode, and much effort has been devoted to encapsulating sulfur in some forms of conductive nanostructures.[24−26] However, loss of polysulfides into the electrolyte may not be the sole reason contributing to capacity decay. In operando transmission X-ray microscopy imaging indicated that dissolution of sulfur into electrolyte was not as severe as previously expected.[27] Ex-situ study involving electrolytes analysis by inductively coupled plasma-optical emission spectroscopy (ICP-OES) has also shown a relatively constant polysulfides concentration in the electrolytes over cycling,[28] despite significant capacity decay. The TEM study here reveals valuable insight into the nanoscale interaction in the electrode, suggesting that sulfur cathode degradation is a multifaceted problem that requires rational design at different length scales: (1) Proper functional groups are needed to modify the interface between the carbon and sulfur in order to stabilize the discharge products. The chemical moieties need to have good binding strength with both the highly polar lithium sulfide and the nonpolar carbon surface. (2) The contact surface area between sulfur and the electrolyte should be minimal to reduce the mobility of lithium polysulfide within the carbon matrix. (3) Sulfur should be evenly distributed in the electrode to prevent inhomogeneous precipitation of lithium sulfide.

Following these guiding principles, we investigated the effect of adding amphiphilic polymers in modifying the interface between sulfur and the hollow carbon nanofiber. We chose polyvinylpyrrolidone (PVP) due to its simple molecular structure and availability. Also, PVP is known to have strong binding with carbon surface from aqueous solution,[29,30] due to the strong thermodynamic driving force in eliminating the hydrophobic interface. We computed the binding energy between Li_xS clusters and the functional groups of the added polymers. In this case, *N*-methyl-2-pyrrolidone (NMP) is used

dx.doi.org/10.1021/nl304795g | *Nano Lett.* XXXX, XXX, XXX−XXX

as the modeling molecule to represent the functional groups in PVP. The results show that Li atoms in Li_xS compounds can always bind to oxygen atom in the organic molecules (bond length ~1.85−1.89 Å), giving high binding energies of 1.29 and 1.01 eV for the LiS-NMP and Li_2S-NMP systems respectively (Figure 3a). In general, oxygenated groups exhibit much higher binding strength with Li_xS compounds. In addition, the hydrophobic groups in PVP allow anchoring of the polysulfides species within the carbon matrix (Figure S4b, Supporting Information). Figure 3b illustrates how the presence of polymer in the hollow carbon nanofiber can improve the cathode performance by retaining lithium sulfide in close proximity to the carbon surface.

Amphiphilic Modification of Electrode. To introduce the polymer, 2 mL of PVP (MW = 55000) solution in methanol was added to the carbon coated anodized aluminum oxide (AAO) template and the mixture was sonicated for about 5 min. The AAO template was then retrieved and rinsed with water to remove the excess solvent. The change in the mass of the AAO tempate after polymer funcionalization was measured (Sartorius SE2 Ultra Micro Balance) and the amount of PVP added into the hollow carbon nanofiber was around 50 μg. Sulfur was infused into the hollow carbon nanofibers using the same method as above. The AAO template was then etched away to form the polymer modified sulfur cathode (Figure S4a, Supporting Information). Figure 3c shows the TEM image of the polymer modified hollow carbon fiber after sulfur infusion. The yellow line represents the EDS counts of sulfur signal across the nanofiber. The sulfur cathode was tested in a 2032-type coin cell with the same parameters as above.

The discharge voltage profile of the polymer modified sulfur cathode is similar to the unmodified structure (Figure S5, Supporting Information). Figure 3d shows the TEM image of the sulfur cathode after discharge to 1.7 V and resting for 24 h. The TEM image of the discharge cathode did not show detachment of lithium sulfide from the carbon surface. The small spots (Figure 3d and Figure S4c (Supporting Information)) suggest that localized detachment of lithium sulfide could still occur. Nevertheless, the integrity of sulfur cathode indicates the polymer has been effective in stabilizing the polysulfides within the carbon nanofiber, preventing the segregation of lithium sulfide from the carbon surface.

Electrochemical Performance. The electrochemical performance of the modified hollow carbon nanofiber/sulfur cathode showed marked improvement as compared to previous result. Figure 4a shows the rate capability performance of the modified sulfur cathode. At *C*/5, a specific capacity of around 1180 mAh/g was achieved. The specific capacities were around 920 mAh/g and 820 mAh/g at *C*/2 and 1*C*, respectively. The voltage hysteresis also decreased from about 350 mV at 1*C* to about 180 mV at *C*/5 (Figure 4d). When the current rate was switched from *C*/5 to *C*/2 at the 40th cycle, the specific capacity at *C*/2 is slightly higher than before from 10th to 20th cycle (Figure 4a). The slight capacity loss observed during cycling is not permanent. In a separate cycling test, the cell was stopped after 80 cycles of charge/discharge and allowed to rest for about 24 h (Figure S6, Supporting Information). The galvanostatic cycling was then restarted at the same *C* rate. The cycling data shows that the specific capacity increases about 7% after the resting. The reversible capacity loss could be due to the excess precipitation of insulating lithium sulfide, which becomes electrochemically inaccessible on the electrode. When the cell was switched to low *C* rate or temporarily stopped, the

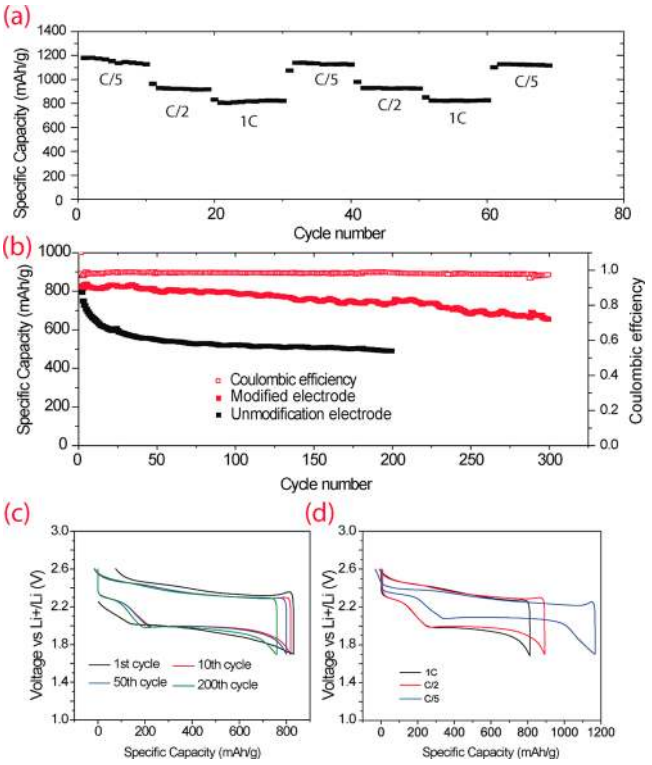

Figure 4. Electrochemical performance of the modified hollow carbon nanofiber cathode. (a) Specific capacities of the PVP modified sulfur cathode at *C*/5, *C*/2 and 1*C* cycling rates. (b) Comparison of cycling performance at *C*/2 with and without the PVP modification. (c) Galvanostatic charge/discharge voltage profiles of the cathode at *C*/2 for the 1st, 10th, 50th, and 200th cycles. (d) Comparison of voltage profiles for cycling at different *C* rates.

inactive lithium sulfide would react with the polysulfide and become active again.[31] This further confirms that reducing segregation of lithium sulfide in the electrode can play an important role in improving cycling performance. Figure 4b shows the cycling performance of the modified cathode at *C*/2 current rate. Instead of the rapid initial decay generally observed in the unmodified electrodes, the first few cycles showed a slight increase in specific capacity from 828 to 838 mAh/g. The amphiphilic polymers provide anchoring points that allow lithium sulfides to bind strongly with the carbon surface. Subsequent cycles showed very stable performance, with less than 3% decay over the first 100 cycles. The capacity retention was over 80% for more than 300 cycles of charge/discharge, with Coulombic efficiency at around 99%.

Figure 4c shows the voltage profiles of the first, 10th, 50th and 200th cycles at C/2. The first discharge shows a small initial plateau, probably due to the reaction between sulfur and the electrolytes. The voltage profiles from the 10th cycle onward are quite similar to each other. The hysteresis between the charge and discharge cycles also decreases significantly during cycling, which could be due to the mitigation of electrode resistance during cycling.

To demonstrate the general applicability of this electrode modification approach, we tested another common amphiphilic polymer Triton X-100. The cycling test showed nearly 90% capacity retention for over 100 cycles in the stabilized region (Figure 5a). For the simulation of binding energy, dimethyl ether (DME) was used as the modeling molecule to represent the functional group in Triton X-100. The results show that the

dx.doi.org/10.1021/nl304795g | *Nano Lett.* XXXX, XXX, XXX−XXX

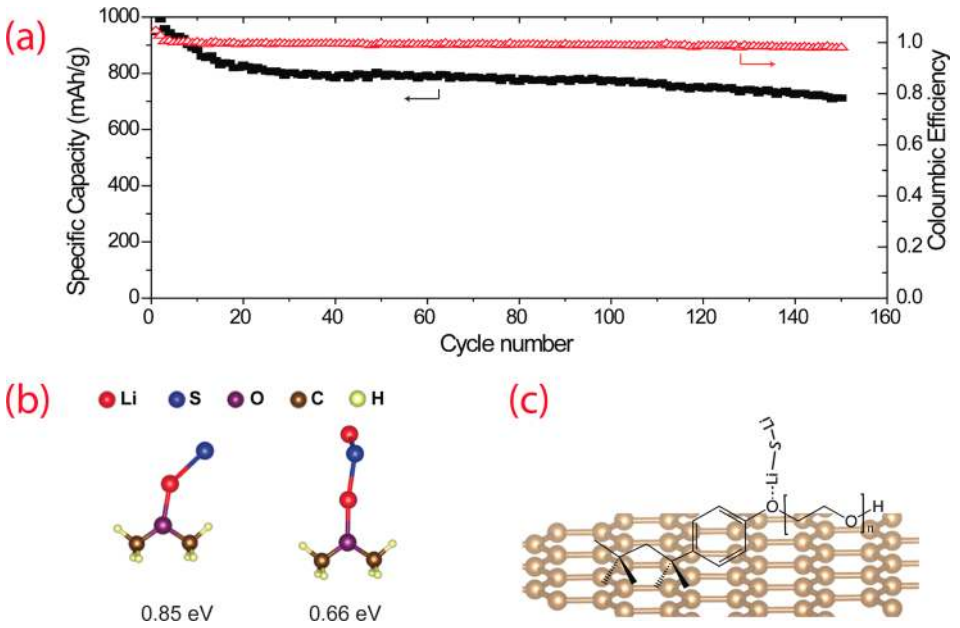

Figure 5. Electrochemical performance and molecular binding models of the sulfur cathode modified with Triton-X100. (a) Cycling performance of sulfur cathode modified with Triton X-100. (b) Molecular models for the interaction between the lithium sulfide clusters, LiS (left) and Li_2S (right), and the DME molecule. (c) Schematic showing the effect of Triton X-100 in facilitating the binding of lithium sulfide to the carbon surface.

binding energy between the Li atom and the oxygen in the ether group is 0.85 and 0.66 eV for LiS-DME and Li_2S-DME, respectively (Figure 5b). These binding energy are slightly lower than that in the PVP system, as reflected by the faster capacity decay. Overall, the presence of amphiphilic polymer helps enhance the interfacial binding between the discharged sulfur and the carbon (Figure 5c).

In summary, we have identified that detachment of lithium sulfide from the carbon surface can be an important contributing factor to the initial capacity decay observed in lithium sulfur batteries. Interfacial modification of carbon with amphiphilic polymers helps stabilize the discharge products and improve the cycling performance. We demonstrated that the modified sulfur cathode could achieve stable performance of more than 300 cycles with 80% capacity retention.

■ ASSOCIATED CONTENT

Supporting Information

Computational methods, fabrication of electrode, modification of electrode interface, characterization, electrochemical testing, and figures showing the fabrication of the sulfur cathode, discharge profile of unmodified electrode, TEM image of sulfur cathode after discharge, fabrication of PVP modified sulfur cathode, discharge profile of the modified sulfur cathode, and cycling performance of the modified sulfur cathode. This material is available free of charge via the Internet at http://pubs.acs.org.

■ AUTHOR INFORMATION

Corresponding Author

*E-mail: yicui@stanford.edu.

Author Contributions

G.Z. and Y.C. conceived the idea. G.Z. carried out materials synthesis and electrochemical tests. Q.Z. carried out theoretical calculation. G.Z. and J.J.C. performed materials characterization. Y.Y., Z.S, and W.L. contributed to the discussion of the results. G.Z. and Y.C. cowrote the paper. All authors commented on the manuscript.

Notes

The authors declare no competing financial interest.

■ ACKNOWLEDGMENTS

This work was supported by the Department of Energy, Office of Basic Energy Sciences, Division of Materials Sciences and Engineering, under Contract DE-AC02-76SF0051, through the SLAC National Accelerator Laboratory LDRD project. G.Z. and Z.W.S acknowledge financial support from Agency for Science, Technology and Research (A*STAR), Singapore.

■ REFERENCES

(1) Bruce, P. G.; Freunberger, S. A.; Hardwick, L. J.; Tarascon, J.-M. *Nat. Mater.* **2012**, *11*, 19.
(2) Yang, Y.; McDowell, M. T.; Jackson, A.; Cha, J. J.; Hong, S. S.; Cui, Y. *Nano Lett.* **2010**, *10*, 1486.
(3) Tarascon, J. M.; Armand, M. *Nature* **2001**, *414*, 359.
(4) Yang, Y.; Zheng, G.; Cui, Y. *Chem. Soc. Rev.* **2013**, DOI: 10.1039/C2CS35256G.
(5) Xiulei, J.; Linda, F. N. *J. Mater. Chem.* **2010**, *20*, 9821.
(6) Mikhaylik, Y. V.; Akridge, J. R. *J. Electrochem. Soc.* **2004**, *151*, A1969.
(7) Ji, X. L.; Lee, K. T.; Nazar, L. F. *Nat. Mater.* **2009**, *8*, 500.
(8) Schuster, J.; He, G.; Mandlmeier, B.; Yim, T.; Lee, K. T.; Bein, T.; Nazar, L. F. *Angew. Chem., Int. Ed.* **2012**, *51*, 3591.
(9) Jayaprakash, N.; Shen, J.; Moganty, S. S.; Corona, A.; Archer, L. A. *Angew. Chem., Int. Ed.* **2011**, *123*, 6026.
(10) Kim, J.; Lee, D.-J.; Jung, H.-G.; Sun, Y.-K.; Hassoun, J.; Scrosati, B. *Adv. Funct. Mater.* **2012**, DOI: 10.1002/adfm.201200689.
(11) Zheng, G.; Yang, Y.; Cha, J. J.; Hong, S. S.; Cui, Y. *Nano Lett.* **2011**, *11*, 4462.
(12) Guo, J.; Xu, Y.; Wang, C. *Nano Lett.* **2011**, *11*, 4288.
(13) Elazari, R.; Salitra, G.; Garsuch, A.; Panchenko, A.; Aurbach, D. *Adv. Mater. (Weinheim, Ger.)* **2011**, *23*, 5641.
(14) Ji, L.; Rao, M.; Zheng, H.; Zhang, L.; Li, Y.; Duan, W.; Guo, J.; Cairns, E. J.; Zhang, Y. *J. Am. Chem. Soc.* **2011**, *133*, 18522.

(15) Wang, H.; Yang, Y.; Liang, Y.; Robinson, J. T.; Li, Y.; Jackson, A.; Cui, Y.; Dai, H. *Nano Lett.* **2011**, *11*, 2644.
(16) Ji, X.; Evers, S.; Black, R.; Nazar, L. F. *Nat. Commun.* **2011**, *2*, 325.
(17) Evers, S.; Yim, T.; Nazar, L. F. *J. Phys. Chem. C* **2012**, *116*, 19653.
(18) Demir-Cakan, R.; Morcrette, M.; Nouar, F.; Davoisne, C.; Devic, T.; Gonbeau, D.; Dominko, R.; Serre, C.; Feryey, G.; Tarascon, J.-M. *J. Am. Chem. Soc.* **2011**, *133*, 16154.
(19) Fu, Y.; Su, Y.-S.; Manthiram, A. *ACS Appl. Mater. Interfaces* **2012**, *4*, 6046.
(20) He, X.; Ren, J.; Wang, L.; Pu, W.; Jiang, C.; Wan, C. *J. Power Sources* **2009**, *190*, 154.
(21) Elazari, R.; Salitra, G.; Talyosef, Y.; Grinblat, J.; Scordilis-Kelley, C.; Xiao, A.; Affinito, J.; Aurbach, D. *J. Electrochem. Soc.* **2010**, *157*, A1131.
(22) Cheon, S.-E.; Ko, K.-S.; Cho, J.-H.; Kim, S.-W.; Chin, E.-Y.; Kim, H.-T. *J. Electrochem. Soc.* **2003**, *150*, A796.
(23) Yuan, L.; Qiu, X.; Chen, L.; Zhu, W. *J. Power Sources* **2009**, *189*, 127.
(24) Manthiram, A.; Fu, Y.; Su, Y.-S. *Acc. Chem. Res.* **2012**, DOI: 10.1021/ar300179v.
(25) Evers, S.; Nazar, L. F. *Acc. Chem. Res.* **2012**, DOI: 10.1021/ar3001348.
(26) Yang, Y.; Yu, G.; Cha, J. J.; Wu, H.; Vosgueritchian, M.; Yao, Y.; Bao, Z.; Cui, Y. *ACS Nano* **2011**, *5*, 9187.
(27) Nelson, J.; Misra, S.; Yang, Y.; Jackson, A.; Liu, Y.; Wang, H.; Dai, H.; Andrews, J. C.; Cui, Y.; Toney, M. F. *J. Am. Chem. Soc.* **2012**, *134*, 6337.
(28) Diao, Y.; Xie, K.; Xiong, S.; Hong, X. *J. Electrochem. Soc.* **2012**, *159*, A421.
(29) Fujita, N.; Asai, M.; Yamashita, T.; Shinkai, S. *J. Mater. Chem.* **2004**, *14*, 2106.
(30) O'Connell, M. J.; Boul, P.; Ericson, L. M.; Huffman, C.; Wang, Y.; Haroz, E.; Kuper, C.; Tour, J.; Ausman, K. D.; Smalley, R. E. *Chem. Phys. Lett.* **2001**, *342*, 265.
(31) Yang, Y.; Zheng, G.; Misra, S.; Nelson, J.; Toney, M. F.; Cui, Y. *J. Am. Chem. Soc.* **2012**, *134*, 15387−15394.